



**HAL**  
open science

# Mode I and II R-curves characterization of the Maritime Pine and Spruce under the same geometry

Edouard Sorin, Jean-Luc Coureau, Cédric Pérez

## ► To cite this version:

Edouard Sorin, Jean-Luc Coureau, Cédric Pérez. Mode I and II R-curves characterization of the Maritime Pine and Spruce under the same geometry. *Engineering Fracture Mechanics*, 2022, 269, pp.108472. 10.1016/j.engfracmech.2022.108472 . hal-03776971

**HAL Id: hal-03776971**

**<https://hal.science/hal-03776971>**

Submitted on 22 Jul 2024

**HAL** is a multi-disciplinary open access archive for the deposit and dissemination of scientific research documents, whether they are published or not. The documents may come from teaching and research institutions in France or abroad, or from public or private research centers.

L'archive ouverte pluridisciplinaire **HAL**, est destinée au dépôt et à la diffusion de documents scientifiques de niveau recherche, publiés ou non, émanant des établissements d'enseignement et de recherche français ou étrangers, des laboratoires publics ou privés.



Distributed under a Creative Commons Attribution - NonCommercial 4.0 International License

# 1 Mode I and II R-curves characterization of the Maritime Pine and 2 Spruce under the same geometry

3 Edouard Sorin<sup>a,\*</sup>, Jean-Luc Coureau<sup>a,\*\*</sup> and Cédric Pérez<sup>a</sup>

4 <sup>a</sup>Université de Bordeaux, UMR 5295, Institut de Mécanique et d'Ingénierie - Bordeaux (I2M), Dépt. Génie Civil et Environnemental (GCE),  
5 Bordeaux F-33000, France

## 8 ARTICLE INFO


## ABSTRACT

10 *Keywords:*  
11 R-curve  
12 Wood  
13 Mode I  
14 Mode II  
15 Fracture Mechanics  
16 Quasi-brittle

This study provides detailed data on the quasi-brittle behaviour of two softwood species, the Maritime Pine (*Pinus pinaster.*) and the Spruce (*Picea abies.*), by using R-curves. The methodology of characterization of the R-curve used in this article is an improvement of the method presented by Lespine [25]. This method is automated and based on the measurement error made on  $G_R(\Delta a_u)$ . And the same geometry to characterize the crack propagation in mode I and in mode II. The influence of the crack plane orientation and the density on the fracture mechanisms is investigated for both species and shows a dependency of the R-curve parameters of the Maritime Pine in mode I to the crack plane orientation. The differences between Spruce and Maritime Pine are highlighted. This demonstrate the importance to characterize the quasi-brittle behaviour of each wood species in order to provide a useful data base for engineers.

## 21 Nomenclature

22  $a_0$  initial crack length  
23  $b$  width of the specimen  
24  $f_t$  tensile strength  
25  $G_{exp}$  experimental crack propagation resistance  
26  $G_f$  cohesive fracture energy  
27  $G_{fb}$  crack bridging energy  
28  $G_{fv}$  microcracking energy  
29  $G_R$  crack propagation resistance  
30  $G_{R_c}$  critical crack propagation resistance  
31  $G_{R_{c_i}}$  critical crack propagation resistance for mode i  
32  $K_{ini}$  initial stiffness  
33  $P$  load applied to specimen  
34  $P_u$  ultimate load  
35  $P.U$  ultimate load  
36  $\beta$  factor which described the damage regime of the R-curve  
37  $\beta_i$  value of  $\beta$  for mode i  
38  $\Delta a$  crack length  
39  $\Delta a_{c_i}$  critical crack length for mode i  
40  $\Delta a_{eq}$  equivalent crack length  
41  $\gamma$  annual growth ring orientation  
42  $\kappa_{G_{R_{err}}}$  measurement error on the experimentam crack propagation resistance  
43  $\lambda$  compliance of the specimen  
44 CZM Cohesive Zone Model  
45 FPZ Fracture Process Zone  
46 LTENF Linear Tapered End Notched Flexure  
47 MC% Moisture Content

 [edouard.sorin@gmail.com](mailto:edouard.sorin@gmail.com) (E. Sorin); [jean-luc.coureau@u-bordeaux.fr](mailto:jean-luc.coureau@u-bordeaux.fr) (J. Coureau)  
ORCID(s):

## 48 1. Context

49 In order to improve the design methods for structural timber elements subjected to splitting, the damage and crack  
 50 propagation mechanisms should be taken into account accurately by using specified mechanical properties. For this,  
 51 in 1988, Gustafsson [18] provides a method to predict the load-bearing capacity of wooden notched beams based  
 52 on the linear elastic fracture mechanics. This method was then implemented in Eurocode 5 [16] with parameters  
 53 determined according to the current knowledge mainly based on the Spruce (*Picea abies.*) properties [1]. Nowadays,  
 54 the knowledge focused on failure mechanism of wood has improved significantly, but the standards and design rules  
 55 still remain the same.

56 However, recent studies demonstrate some limits of the current design method. First of all, in these methods the  
 57 wood is considered as a perfectly brittle material with no transition phase between its elastic behaviour and the crack  
 58 propagation, because only the critical crack propagation resistance is considered to estimate the ultimate load of the  
 59 structural elements. But, some experiments reveal that a transition phase does exist with no plasticity and demonstrate  
 60 the quasi-brittle behaviour of wood [28]. In this case, considering wood as a perfectly brittle material can lead to an  
 61 overestimation of the load-bearing capacity ; because the progressive damaging of the element before the auto-similar  
 62 crack propagation is not taken into account [7].

63 Secondly, the crack propagation in mode I is the most investigated one, whereas recent studies based on digital  
 64 correlation measurements of strain fields clearly show the influence of the crack propagation in mode II for notched  
 65 beams [20, 34]. The mode I is an opening of the crack due to tensile stress. The mode II is the propagation of the crack  
 66 caused by in plane shear stress and the mode III is the one due to out of plane shear stress also named tearing.

67 Finally, the parameters used in the Eurocode 5 were calibrated mainly on the Spruce properties by assuming a  
 68 correlation between the wood density and the fracture properties. But the literature shows that the failure properties  
 69 are very different from a species to another one [15], and a correlation between the wood density and the fracture  
 70 properties is not always found and accurate [21].

71 Currently, the literature presents some experimental investigations carried out to determine the mechanical prop-  
 72 erties governing the damage and failure of wood in mode II [1, 13, 35, 37], but these works are much scarcer in  
 73 comparison with those in mode I. Some studies were also conducted to determine the fracture properties of wood  
 74 in mixed-mode [12, 19, 26, 36] but these works are even scarcer than the one in mode II. However, recent stud-  
 75 ies [20, 23, 33, 34] demonstrate that the splitting of wood in structural elements is mostly governed by the combination  
 76 of mode I and II, with a non negligible contribution of the mode II. So, as a revision of the Eurocode 5 is conducted [14],  
 77 the design methods of the structural elements submitted to splitting should be investigated again in order to consider  
 78 the latest knowledge relative to the crack propagation in wood. This implies experimental campaigns rigorously chosen  
 79 in order to characterise the degree of anisotropy of the failure properties. So, this study presents a methodology and  
 80 the corresponding results to supply additional knowledge relative to the failure mechanisms of wood.

81 The quasi-brittle behaviour of the wood is due to the presence of a damaged area in front of the "visible" crack  
 82 tip [28]. This area is named Fracture Process Zone (FPZ) and presents micro-cracking and crack bridging. The FPZ  
 83 may measure several centimetres. This local damage should be well considered because it produces a progressive  
 84 decrease of the local stress transfer which can lead to the sudden failure of the structural element. In this case, a design  
 85 method based on the brittleness assumption might overestimate the load-bearing capacity of the structural element.  
 86 This particularity of the wood has been studied since several years [10, 11, 28]. However the phenomenon is still  
 87 not currently considered in the design methods. Some studies considered the quasi-brittleness of the wood to design  
 88 structural element [5, 8, 17] but they used non-linear models which are too specific and too greedy in numerical  
 89 resources, limiting their uses by engineers. Moreover, the fracture properties implemented in those models are not  
 90 based on dedicated experimental campaigns, while size effects and boundary conditions may influence the results [4].

91 In order to consider the quasi-brittle behaviour of wood without the inconvenient of the non-linear models, some  
 92 studies [24, 33] used Equivalent Linear Elastic Fracture Mechanics ( $_{eq}$ LEFM) proposed by Bazant [2, 3] and applied  
 93 to wood by Morel [28]. This method considers the damage of the material by using an equivalent crack length ( $\Delta a_{eq}$ )  
 94 able to reproduce the FPZ development , and the auto-similar crack propagation according to the compliance evolution  
 95 of the specimen. This leads to the determination of the crack resistance propagation function ( $G_R$ ) according to the  
 96 equivalent crack length, which is an R-curve. This one depends on the material, and is regarded as a fracture property of  
 97 the material. So, with the  $_{eq}$ LEFM, the progressive failure of the specimen during the damage phase can be considered  
 98 by using R-curves which are more elaborated and complete than the fracture energy ( $G_f$ ) [18] only.

99 However, the R-Curve characterization implies to obtain experimentally a stable phenomenon from damage initi-

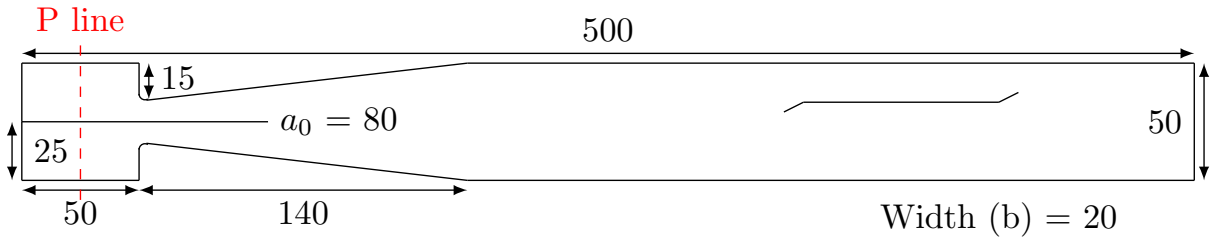


Figure 1: Schema of the specimen geometry (LTENF) with dimensions in mm

100 ation to the auto-similar propagation of the crack. But, in the literature, several specimen geometries have too short  
 101 ligament (CT, SENB for instance) to reach the critical energy release rate corresponding to the fracture energy [6]. And,  
 102 although the R-curve is a material property, its characterization is dependent on the specimen geometry [3, 27, 30]. This  
 103 dependence is supposed to be linked to the average compliance of the specimen. This can explain the differences in the  
 104 fracture properties proposed by the literature [15, 25, 28, 32, 35], which complicates the comparison between studies.  
 105 All those specificities imply that the choice of the specimen geometry used to characterize the fracture properties is cru-  
 106 cial for quasi-brittle material. Moreover as the wood is an orthotropic material with three principal orientation (radial  
 107 (R), tangential (T) and longitudinal (L)) the crack plane orientation can have an influence one the fracture properties.  
 108 Two crack planes orientation (RL) for Radial/Longitudinal and (TL) for Tangential/Longitudinal were investigated. In  
 109 those cases the crack propagates along the longitudinal direction in parallel (RL) or in perpendicular (TL) to annual  
 110 growth rings as shown by figure 2.

111 The R-curves describe the FPZ development which is governed by the geometry, the elastic properties and the  
 112 mode of crack propagation. So, to predict the failure of structural elements subjected to splitting, where cracks are  
 113 developing due to mode I and II [9, 20, 34], the R-curves of each mode must be characterized.

114 The main goal of the current study is to provide fracture properties of Spruce (*Picea abies.*) and Maritime Pine  
 115 (*Pinus pinaster.*) for mode I and mode II using the same specimen geometry. The interest is to avoid geometry and size  
 116 effect dependence, of fracture properties. In a second time, the study aims at providing data of the fracture properties  
 117 of Maritime Pine and Spruce for mode I and II crack propagation according to the orthotropy of the wood. Thus,  
 118 correlations between R-Curves and the wood density or the annual growth rings orientation (from RL to TL) are  
 119 proposed.

## 120 2. Methods

### 121 2.1. Specimens characteristics

122 The selected fracture specimen geometry (named LTENF) (Figure 1) was taken from a previous experimental  
 123 campaign carried out by Aicher *et al.* [1]. The P line represents the loading line for mode I test and the center of the  
 124 support for the mode II test, the value of  $a_0$  is given from this line. It was mainly used for mode II characterization  
 125 of wood as a brittle material. This specific geometry was chosen because it ensure a stable crack propagation near the  
 126 initial crack ( $a_0$ ) and during all the microcracking process, which can be of many centimetres for some wood species,  
 127 like the Maritime Pine. This stability is crucial to characterize the fracture properties of quasi-brittle material. In order  
 128 to take into account the geometry specificities and to avoid uncertainties on the calculation of the energy release rate,  
 129 the evolution of the compliance of the specimen was computed using a finite element model. Others geometries in the  
 130 literature, like de ENF or DCB, do not provide stable cracking for the mode I and the mode II unless the mechanic press  
 131 is very specially monitored. Which is more difficult and expensive in raw materials than using a finite element model  
 132 in place of the beam theory. A geometry presenting a similar slenderness ratio was used by Phan [31] to characterize  
 133 the mode I R-curve of Maritime Pine.

134 In order to be representative of the wood variability 92 tests were carried out for Maritime Pine and 90 for Spruce.  
 135 The crack propagation plane orientation [1] goes from RL to TL with a quiet homogeneous repartition of the tests.  
 136 This orientation was determined by image analysis for every specimen tested (Figure 2). The picture was taken in order  
 137 to be perpendicular with the crack propagation direction. The annual growth ring orientation was determined as the

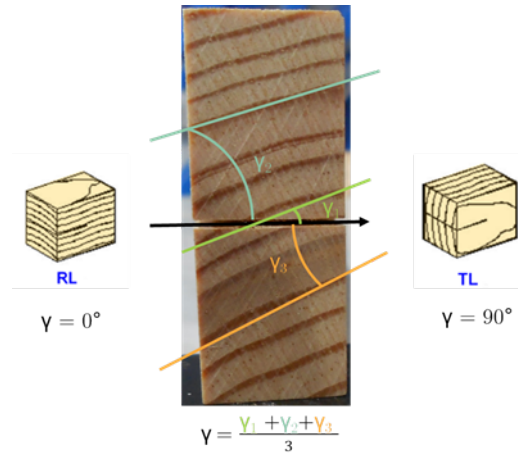


Figure 2: Measurement of the annual growth ring orientation ( $\gamma$ ) of a test specimen



Figure 3: Opening test for mode I

138 mean value of three annual growth ring orientation present on ( $\gamma_1$ ), below ( $\gamma_2$ ) and under ( $\gamma_3$ ) the crack path.

139 Free-defect specimens were chosen to avoid the heterogeneities on the supposed crack path and to privilege a  
 140 straight wood grain. The wooden pieces were previously conditioned to a temperature of 20°C and a relative humidity  
 141 of 65% to obtain a moisture content close to 12%. The average density at a moisture content of 12% is equal to 470  
 142  $kg/m^3$  for the Spruce and 570  $kg/m^3$  for the Maritime Pine.

## 143 2.2. Test protocol

144 The mechanical characterizations were carried out on a 50 kN MTS criterion electro-mechanic press (MTS Sys-  
 145 tems). Experiments in mode I consist in an opening test (Figure 3) and the corresponding mode II is a 3 points flexion  
 146 test (Figure 4).

147 For each test the same protocol was strictly followed. First, the initial notch was realised at the earliest 48 hours  
 148 before the test. Then a little knife cut was performed just before the test beginning (1 mm long). The controlled  
 149 displacement of the test was determined according to the wood species in order to ensure a short time protocol between  
 150 3 and 7 minutes. After each failure of the specimens, the moisture content (MC%) was measured as well as the local  
 151 density on the observed crack path at MC% = 12% and MC% = 0% (anhydrous state). The moisture measurements were  
 152 carried out according to the ISO-13061-1 standard, this standard is not official for research, and the weighing material  
 153 was calibrated. The objective of these tests is to measure the compliance variation due to the damage development and  
 154 the potential crack extension of the specimen, which can be done by using the load-displacement curve (Figure 5(a)) if  
 155 the displacement is measured on the loading line. For mode I, the compliance relative to the fracture specimen opening  
 156 at the load support is measured by image tracking . For mode II, the displacement is measured using an LVDT fixed  
 157 to a system avoiding the crushing at the supports (Figure 4).

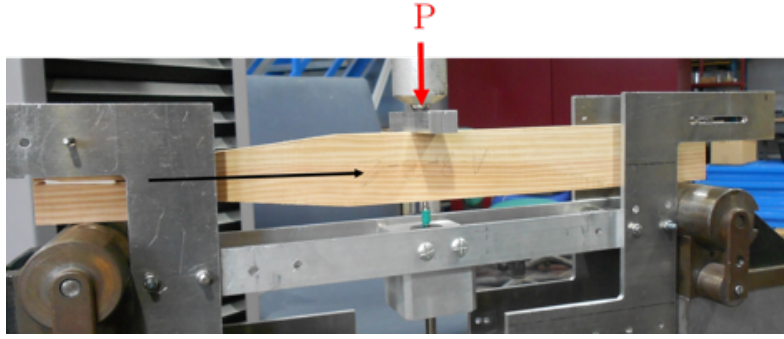


Figure 4: 3-points bending test for mode II

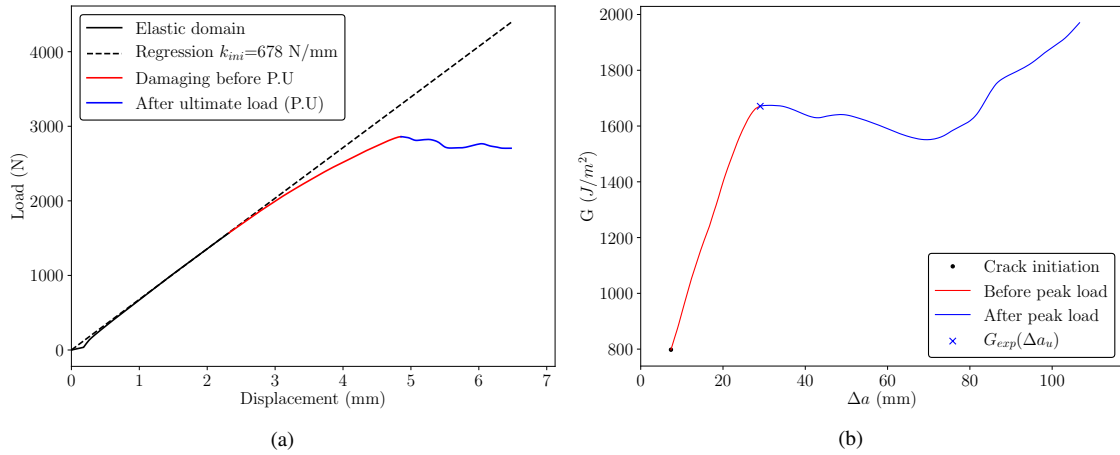


Figure 5: Example of a Load-Displacement curve (a) used to determine the characteristic R-curve (b) of a specimen (Mode II)

### 158 2.3. Experiments

159 In the literature, the cohesive zone models (CZM) are presented as the most efficient method to characterize the  
 160 quasi-brittle behaviour of wood [6, 7, 29]. In order to characterize its corresponding parameters from the R-curves,  
 161 which are determined from the experimental load-displacement curves, a step by step correspondence linking the soft-  
 162 ening function to  $G_R(\Delta a)$  was established by Morel *et al.* [29]. So, the plateau value ( $G_{Rc}$ ) of the R-curve corresponds  
 163 to the cohesive fracture energy ( $G_f$ ), which is the total energy required to completely separate the material in a pure  
 164 mode of failure. The critical equivalent length ( $\Delta a_c$ ) is representative of the FPZ length which is governed by ultimate  
 165 displacement in the material. The parameter  $\beta$  is influenced by the energy distribution between the microcracking en-  
 166 ergy ( $G_{f\mu}$ ) and the crack-bridging energy ( $G_{fb}$ ), the value of  $\beta$  increases when the crack-bridging energy increases [6].  
 167 Finally, the initial part of the R-curve is determined by the tensile strength ( $f_t$ ) of the material which governs the devi-  
 168 ation from the linearity part of the load-displacement curve. So, by this correspondence, the R-curve parameters can  
 169 be linked to the characteristics fracture mechanisms of quasi-brittle materials.

170 In order to determine the experimental crack resistance propagation of a specimen, the relation between the equiv-  
 171 alent crack length ( $\Delta a_{eq}$ ) and the compliance ( $\lambda$ ) must be known. This relation is determined in post-treatment using a  
 172 finite element model. For both tests a numerical model is realised with two calculations each, for each wood species.  
 173 The crack propagation is simulated by the decohesion of the nodes along the crack path. This provides a numer-  
 174 ical relation between the equivalent crack length and the numerical compliance ( $\lambda_n(\Delta a_{eq_n})$ ). Then the experimen-  
 175 tal relation between  $\lambda$  and  $\Delta a_{eq}$  can be determined by a dichotomic approach. However, in order to take into account  
 176 the variability of the elastic properties of wood the numerical relation  $\lambda_n(\Delta a_{eq_n})$  must be corrected by a correction

177 coefficient ( $c_{n/e}$ ). This coefficient is determined by the ratio between the experimental and numerical initial toughness  
 178 ( $K_{ini}$ ) which are only influenced by the elastic properties and the initial state of the test (equation 1).

$$c_{n/e} = \frac{K_{ini_e}}{K_{ini_n}} \quad (1)$$

179 This method was presented by Morel *et al.* [29] and also used by Lespine [25] and Phan [31]. As the relation  
 180 between the experimental compliance ( $\lambda$ ) and the equivalent crack length, noted  $\Delta a$  in the rest of this article, is known,  
 181 the evolution of the experimental crack resistance propagation ( $G_R(\Delta a)$ ) (Figure 5(b)) can be calculated using the  
 182 equation 2 [28]( $P(\Delta a)$  the load and  $b$  the width of the specimen) :

$$G_R(\Delta a) = \frac{P^2(\Delta a)}{2b} \lambda'(\Delta a) \quad (2)$$

183 Equation 2 is only valid in the non-elastic domain. The end of the elastic domain is determined by choosing a load  
 184 value corresponding to the deviation of the load-displacement curve from the initial regression as shown on figure 5(a).  
 185 The end of the elastic domain corresponds to the passage from the black line to the red line.

186 Morel [28] proposed to idealize experimental R-Curves by a 3-parameters power law (Equation 3). Nevertheless,  
 187 this equation can have multiple solutions. So, a strategy of determination is proposed in this study to extract different  
 188 parameters, and detailed below.

$$G_R(\Delta a) = \begin{cases} G_{Rc} \left[ \frac{\Delta a_c}{\Delta a} \right]^\beta & \text{if } \Delta a < \Delta a_c \\ G_{Rc} & \text{if } \Delta a \geq \Delta a_c \end{cases} \quad (3)$$

189 The critical energy release rate or plateau value of the R-curve ( $G_{Rc}$ ) which conditioned the values of the two others  
 190 parameters must be determined at first. Indeed, the critical crack length ( $\Delta a_c$ ) and the damage regime described by ( $\beta$ )  
 191 are dependent of the transition between two energetic states. The undamaged state  $G_R = 0$  and the auto-similar crack  
 192 propagation state  $G_R = G_{Rc}$ , the R-curve ensure the continuity between those states, which govern the process zone  
 193 (FPZ) development. So, the determination of the plateau value on the experimental R-curve leads to the value of  $G_{Rc}$ .

194 In order to connect this value to the experimental reality, it was chosen to consider the measurement errors ( $\kappa_{G_{Rerr}}$ )  
 195 relative to  $G_R$  as a critical parameter of determination. So the plateau of  $G_R(\Delta a)$  was determined by dragging an  
 196 interval from the minimum to the maximum value of the experimental energy release rate ( $G_R$ ) (Figure 6(a)).  $G_{Rc}$   
 197 is the value on which the interval containing the maximum of experimental points is centred. For this experimental  
 198 campaign,  $\kappa_{G_{Rerr}}$  was equal respectively to  $3 \text{ J/m}^2$  for the mode I and to  $30 \text{ J/m}^2$  for the mode II, according to the  
 199 experimental device.

200 Then the critical crack length ( $\Delta a_c$ ) is determined on the curve  $\log(G_R)/\log(\Delta a)$  as the intercept between the  
 201 linear regression of the experimental curve on the interval  $[\log(G_R(0)); \log(G_R(G_{Rc}))]$  with the straight equal to  
 202  $\log(G_R(G_{Rc}))$  (Figure 6(b)). With this method,  $\beta$  is determined from the slope of the linear regression. Nevertheless,  
 203 there is often some noise at the beginning of curve, so, to minimize this influence, the interval of the linear regression  
 204 is reduced to ensure the best regression possible. It is important to notice that the critical crack length is not always  
 205 equal to the ultimate load crack length ( $\Delta a_u$ ) which corresponds to the crack length where the ultimate load ( $P_u$ ) is  
 206 reached.

207 A reverse analysis is then performed by comparing the load-displacement curve generated from the 3-parameters  
 208 R-curve, using equation 4, to the experimental load-displacement curve (Figure 7(a)). The blue dash curve allows  
 209 checking that equation 4 can be used to determine a load-displacement curve from a given R-curve. If the experimental  
 210 load-displacement curve and the blue dash one are equal then equation 4 can be used. The red dash curve represents the  
 211 load-displacement curve obtained by using equation 4 on the 3-parameters R-curve which fitted the experimental curve  
 212 (red dash curve on figure 7(b)). This approach aims at checking if the theoretical R-curve (Figure 7(b)) determined by

## Mode I and II R-curves characterization of the Maritime Pine and Spruce

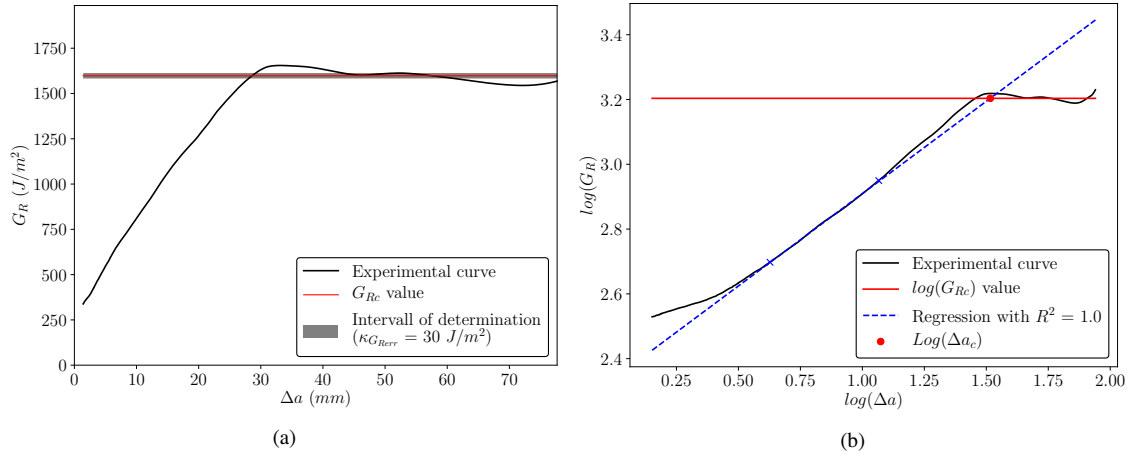


**Figure 6:** Determination of the plateau value ( $G_{Rc}$ ) (a) and linear regression (b) on the  $\log(G_R(\log(\Delta a)))$  function in order to obtain  $\beta$  and  $\Delta a_c$  for the characteristic R-Curve (Mode II)

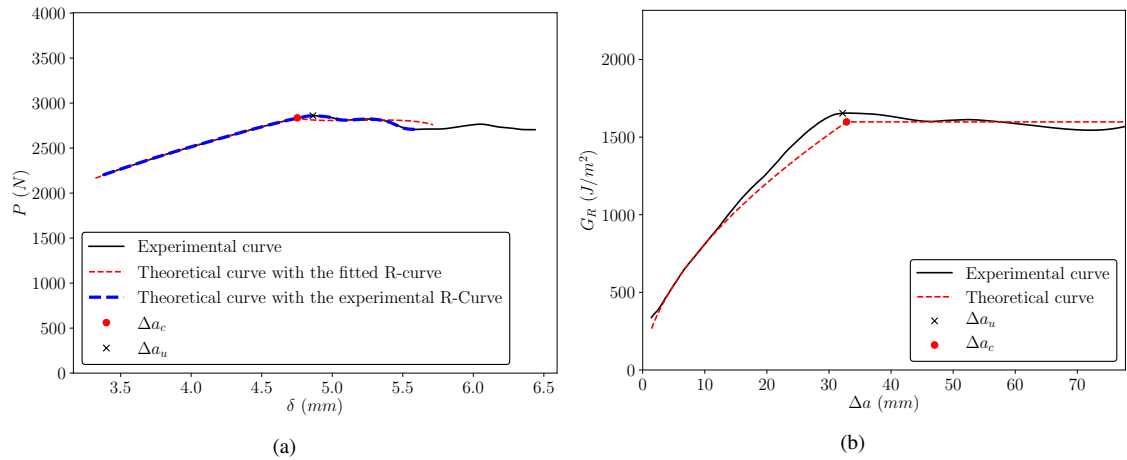


**Figure 7:** Comparison between the non-linear party of the Load-Displacement curves (a) corresponding to the experimental and the fitted R-Curves (b) (Mode II)

213 this method can be used to characterize the fracture properties of the wood.

$$P(\Delta a) = \sqrt{\frac{2bG_R(\Delta a)}{\lambda'(\Delta a)}} \quad (4)$$

214  $P(\Delta a)$  is the load for a given crack length  $\Delta a$ .  $b$  is the specimen width.  $G_R$  is the evolution of the crack resistance  
 215 according to the equivalent crack length  $\Delta a$ . And  $\lambda'(\Delta a)$  is the derivative of the compliance.

### 216 3. Results

217 Some tests were rejected from the final results because no plateau was observed. This can be due to the residual  
 218 presence of knots along the crack path, or a too highly deviation of the wood grain (Figure 8(a)). In the case of mode  
 219 II, this can also be due to a too short ligament of the specimen (Figure 8(b)). Finally, this led to a rejected rate of 15%  
 220 for mode I tests and 30% for mode II.



## Mode I and II R-curves characterization of the Maritime Pine and Spruce

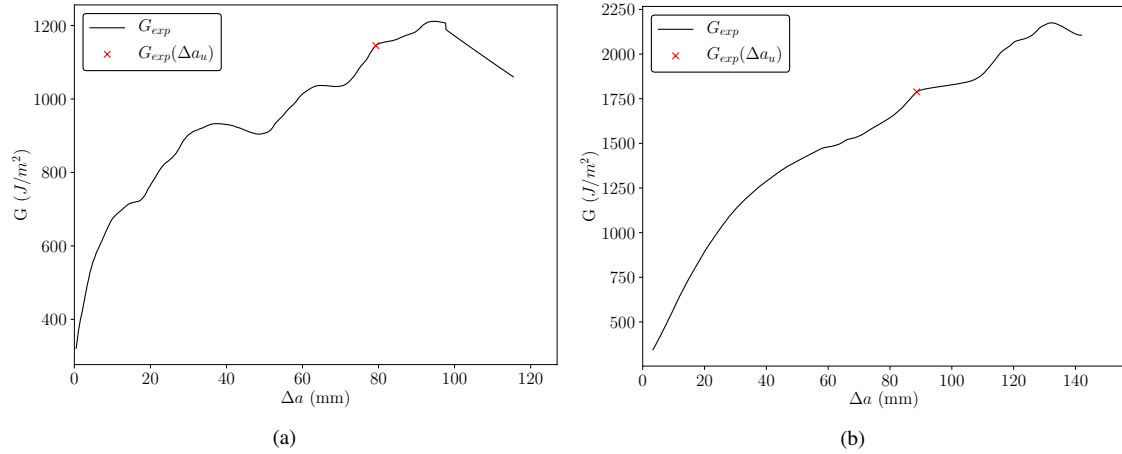


**Figure 8:** Example of an R-Curve with an energy leap (a) (Mode I) and another where the energy release rate constantly increases without reaching a plateau value before failure (b) (Mode II)

**Table 1**

Experimental results for Spruce ( $\rho_{12\%} = 470 \text{ kg/m}^3$ )

Parameters	$G_{RcI}$ $J/m^2$	$G_{RcII}$ $J/m^2$	$\Delta a_{cI}$ (mm)	$\Delta a_{cII}$ (mm)	$\beta_I$ (-)	$\beta_{II}$ (-)
Mean value	190	800	12	22	0.14	0.54
Standard deviation	60	180	8	8	0.06	0.17
CoV	32%	23%	65%	36%	45%	31%

**Table 2**

Experimental results for Maritime Pine ( $\rho_{12\%} = 570 \text{ kg/m}^3$ )

Parameters	$G_{RcI}$ $J/m^2$	$G_{RcII}$ $J/m^2$	$\Delta a_{cI}$ (mm)	$\Delta a_{cII}$ (mm)	$\beta_I$ (-)	$\beta_{II}$ (-)
Mean value	500	1190	24	25	0.25	0.63
Standard deviation	210	275	15	6	0.10	0.10
CoV	43%	23%	61%	22%	41%	16%

### 221 3.1. R-Curve parameters values

222 Table 1 and 2 present the average values of the R-curve parameters in mode I and II for Spruce (*Picea abies.*) and  
223 Maritime Pine (*Pinus pinaster.*).

224 For Spruce, the value obtained for  $G_{RcI}$  ( $190 \text{ J/m}^2$ ) and  $G_{RcII}$  ( $800 \text{ J/m}^2$ ) are similar to the ones of the litera-  
225 ture [15, 25, 32]. But, the critical crack length  $\Delta a_{cI}$  and  $\Delta a_{cII}$  are two times lower than those of the literature [25, 32],  
226 and the value of  $\beta_{II}$  is much higher than  $\beta_I$  which is different from the results of Phan et al. [32].

227 However, the comparison between mode I and mode II parameters exhibits the degree of anisotropy of the material.  
228 The critical energy release rate ( $G_{Rc}$ ) and  $\beta$  are 4 times higher in mode II. A higher  $\beta$  in mode II indicates a significant  
229 crack-bridging in the development of the FPZ. The critical crack length ( $\Delta a_c$ ) is 2 times higher in mode II, so the  
230 failure is more quasi-brittle in mode II than in mode I. With such important differences the mode II crack propagation  
231 should not be ignored for the prediction of structural elements in wood subjected to splitting.

232 For the Maritime Pine the value obtained for  $G_{RcI}$  ( $500 \text{ J/m}^2$ ) is in accordance with the value obtained by Phan [31]

## Mode I and II R-curves characterization of the Maritime Pine and Spruce

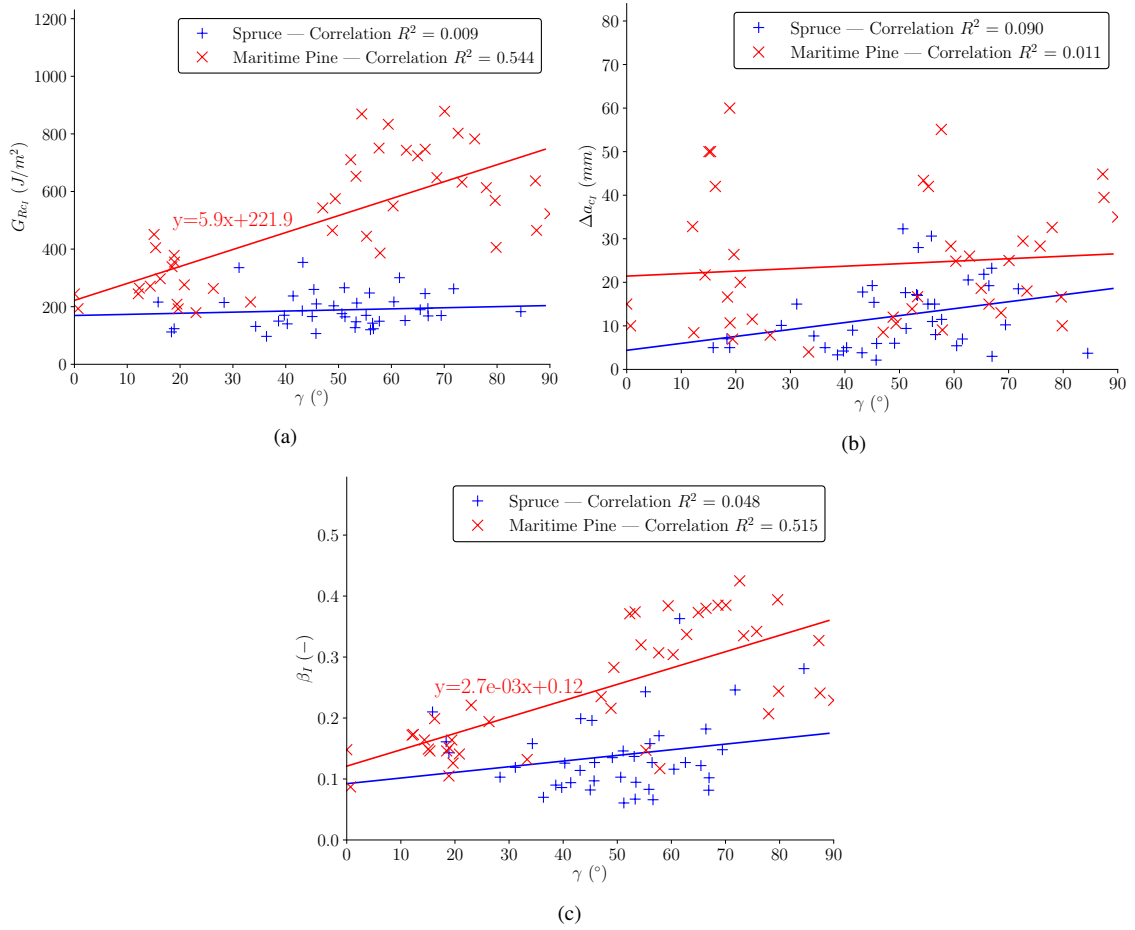


**Figure 9:** Evolution of  $G_{Rc_I}$  (a),  $\Delta a_{c_I}$  (b) and  $\beta_I$  (c) according to the crack orientation plane for both species

233 but higher than the one found by Dourado et al.[15]. The value of  $\Delta a_{c_I}$  is 30% higher than Phan [31] when  $\beta_I$  is similar.  
 234 These differences reveal the importance to propose a retrofitting method to extract the R-curve. The comparison  
 235 between the R-curve parameters in mode I and II shows that  $G_{Rc_{II}}$  and  $\beta_I$  are 2.5 times higher in mode II when  $\Delta a_{c_I}$   
 236 and  $\Delta a_{c_{II}}$  are similar. The lack of data in the literature is significant for the Maritime Pine contrary to the Spruce. This  
 237 highlighted the interest of the present study to supply data on this species. Indeed, the critical energy release rate  $G_{Rc}$   
 238 of the Maritime Pine is 2.5 higher in mode I and 1.5 higher in mode II than the one of the Spruce. So, the Maritime  
 239 Pine is globally more resistant to the crack propagation than the Spruce. Moreover, unlike Spruce, the critical crack  
 240 length are equal in mode I and II for the Maritime Pine.  $\beta_I$  is 2 times higher for the Maritime Pine, but  $\beta_{II}$  is almost  
 241 the same for both species. So, the Maritime Pine is less brittle in mode I, but the mode II crack propagation of both  
 242 species are similar in terms of behaviour.

### 243 3.2. Influence of the crack plane orientation

244 In this part, the influence of the crack plane orientation according to the annual growth ring orientation on the R-  
 245 curve is investigated for both species. The influence on the mode I R-curve parameters is presented on figures 9(a), 9(b)  
 246 and 9(c) and on the figures 10(a), 10(b) and 10(c) for the mode II. When it was relevant the equation of the correlation  
 247 straight line was added to the graphic.

248 Those graphics exhibit an influence on  $G_{Rc_I}$  and  $\beta_I$  for the Maritime Pine, whereas it is not the case for Spruce.  
 249 This leads to values of  $G_{Rc_I}$  and  $\beta_I$  really similar to Spruce for RL ( $\gamma = 0^\circ$ ) orientation, with a  $\Delta a_{c_I}$  2 times higher.  
 250 And for the TL ( $\gamma = 90^\circ$ ) orientation,  $G_{Rc_I}$  and  $\beta_I$  are 4 times higher for the Maritime Pine. So, according to the  
 251 crack plane orientation in mode I, the Maritime Pine can have a significantly higher fracture energy and a less brittle

## Mode I and II R-curves characterization of the Maritime Pine and Spruce

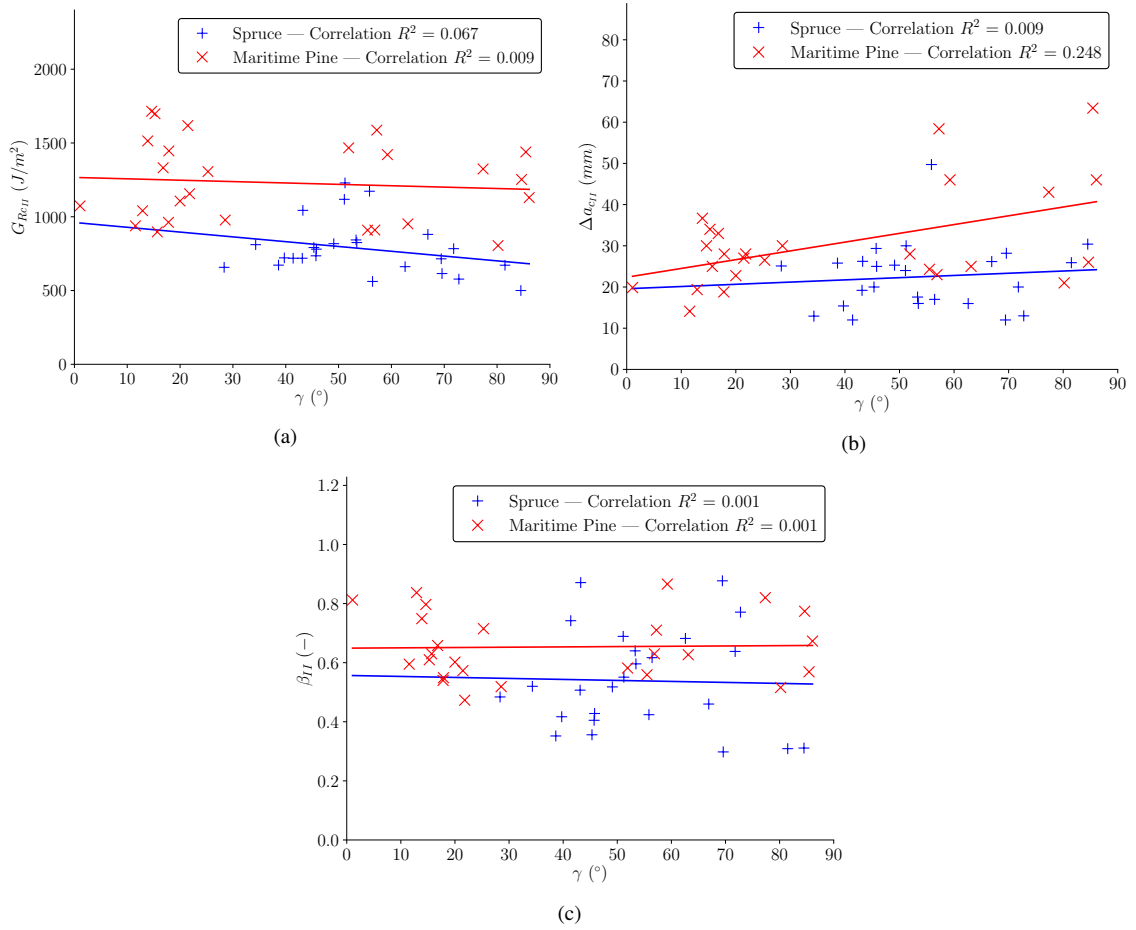


**Figure 10:** Evolution of  $G_{Rc_{II}}$  (a),  $\Delta a_{c_{II}}$  (b) and  $\beta_{II}$  (c) according to the crack orientation plane for both species

252 behaviour than the Spruce.

253 On another hand, the figures 10(a),10(b) and 10(c) that illustrate the influence of the crack plane orientation on the  
 254 R-curve parameters in mode II do not show any significant correlation for both. Moreover,  $\Delta a_{c_{II}}$  and  $\beta_{II}$  are almost  
 255 equal for both species. The differences between those two species are less important in mode II than in mode I, and  
 256 are only obtained for the critical energy release rate ( $G_{Rc_{II}}$ ). Some graphics seem to show some correlation, but as the  
 257  $R^2$  is inferior to 0.5 no conclusion can be made.

### 258 3.3. Influence of the wood density

259 The influence of the wood density on the R-curve parameters is investigated for both species in mode I (Fig-  
 260 ures 11(a),11(b) and 11(c)) and II (Figures 12(a),12(b) and 12(c)). The density of each specimen was measured on  
 261 a cube of approximately 20 mm side taken close to the crack tip after each test. The results are given for a moisture  
 262 content of 12%.

263 For  $G_{Rc_I}$  (Figure 11(a))the values obtained for the Maritime Pine seem to decrease for the highest values of wood  
 264 density, but there is not a clear correlation between these two parameters ( $R^2 < 0.2$ ). The variability is very high and  
 265 does not allow to have a good correlation. It can be a consequence of the crack plane orientation dependence of the  
 266 R-curves parameters in mode I. On another hand, the value obtained for the Spruce, which are not influenced by the  
 267 crack plane orientation, does not show any correlation between  $G_{Rc_I}$  and the wood density too. When both species  
 268 are considered together, the  $R^2$  is inferior to 0.2, which is too low to exhibit any influence of the density on  $G_{Rc_I}$ .  
 269 The influence of the density cannot be decoupled from the influence of the species. For  $\Delta a_{c_I}$  (Figure 11(b)) and  $\beta_{II}$

## Mode I and II R-curves characterization of the Maritime Pine and Spruce

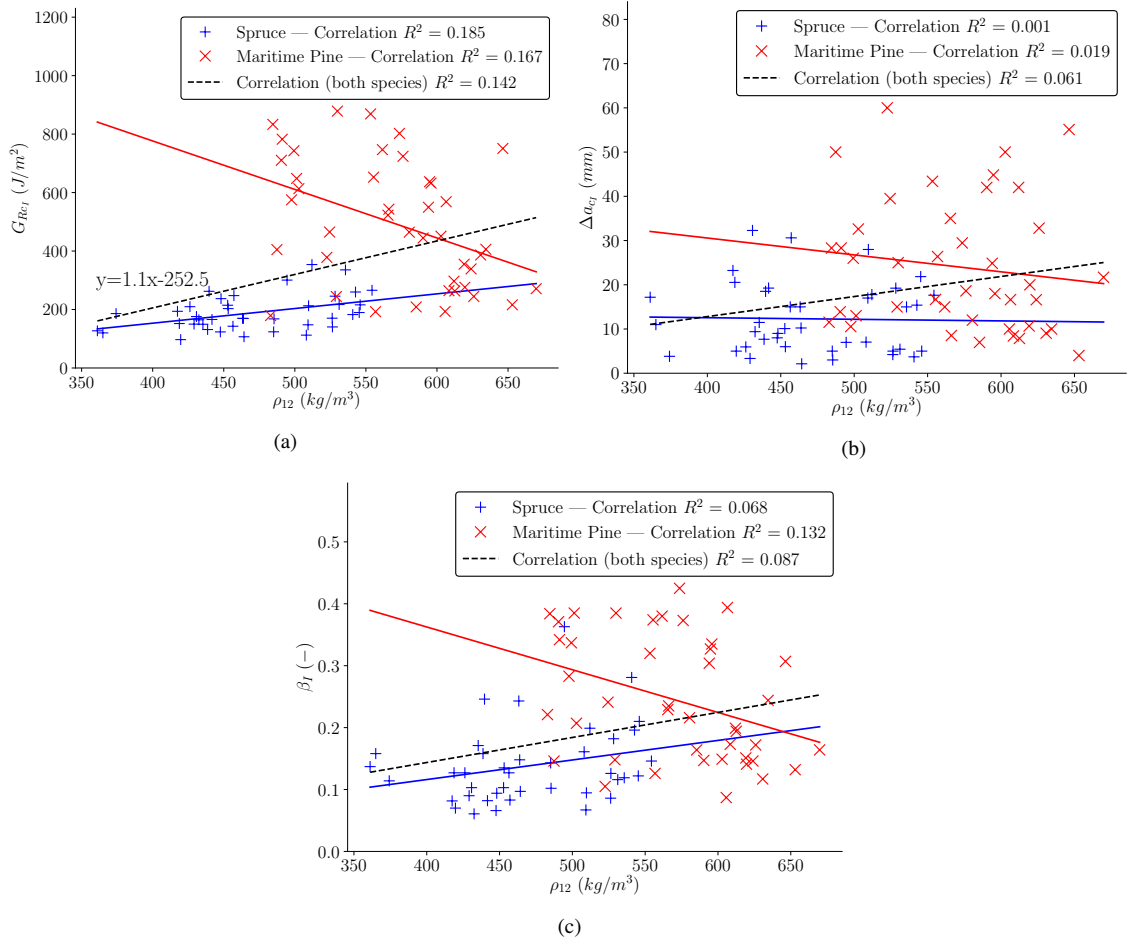


**Figure 11:** Evolution of  $G_{RcI}$  (a),  $\Delta a_{cI}$  (b) and  $\beta_I$  (c) according to the wood density for both species

270 (Figure 11(c)), the variability of the values obtained for both species do not allow to observe any correlation. So, for  
 271 the mode I, the results of the experimental campaign presented in this article does not show any clear influence of the  
 272 wood density on the R-curve parameters for the Spruce and the Maritime Pine.

273 The variability of the R-curve parameters values in mode II is almost the same for both species. This observation  
 274 is in accordance with the assumption that the variability observed, for the Maritime Pine, on the R-curve parameters in  
 275 mode I is due to the influence of the crack plane orientation. For  $G_{RcII}$  (Figure 12(a)) and  $\Delta a_{cII}$  (Figure 12(b)) there is  
 276 no correlation with the wood density for both species. For  $\beta_{II}$  (Figure 12(c)), the values obtained for the Spruce seem  
 277 to increase according to the wood density, but the value of  $R^2$  is inferior to 0.2, so there is no correlation between those  
 278 two parameters. So, even more clearly than for the mode I, there is no influence of the wood density on the R-curve  
 279 parameters in mode II.

280 These results are in accordance with the observation made by Jockwer et al. [21] who question the relation proposed  
 281 by Larsen and Gustafsson [22] which link the fracture energy to the wood density.

282 Figure 13(a) and 13(b) show no correlation between the annual growth ring orientation and the wood density. So  
 283 there is no hidden influence between those two parameters.

## 284 4. Discussions and Conclusions

285 This article proposes a new methodology to characterize the quasi-brittle properties of wood, by using R-curves,  
 286 based on the method presented by Lespine [25]. The main improvement of this methodology compared to Lespine's

## Mode I and II R-curves characterization of the Maritime Pine and Spruce

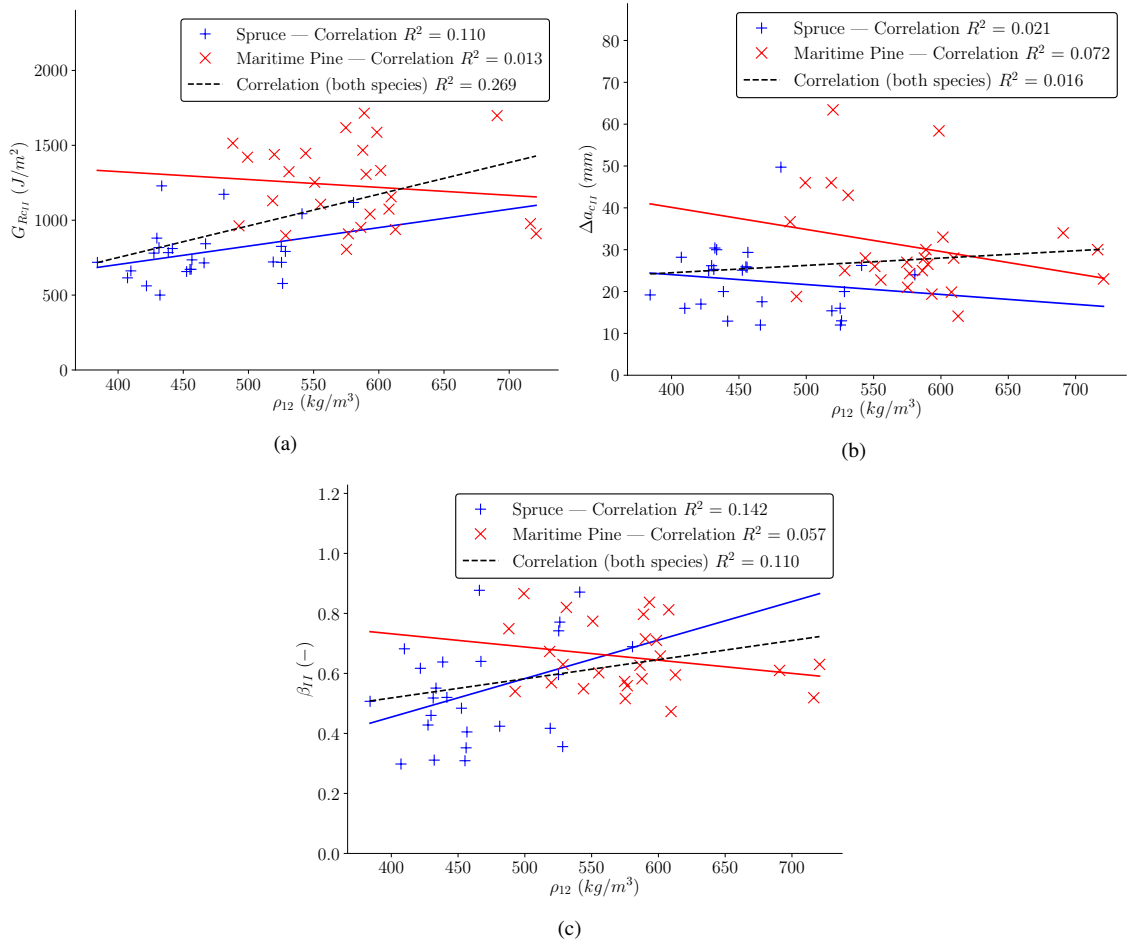


**Figure 12:** Evolution of  $G_{RcII}$  (a),  $\Delta a_{cII}$  (b) and  $\beta_{II}$  (c) according to the wood density for both species

287 one is to automatically determined the plateau value  $G_{Rc}$  by using the measurement error made on  $G_R(\Delta a_u)$ . This  
 288 improves the determination of  $G_{Rc}$ , but also the one of  $\beta$  and  $\Delta a_c$ , which are both strongly linked, to the plateau value  
 289 by preventing mostly the statistical variations in the results induced by the subjectivity of the observer. This method is  
 290 an important step for the characterization of the quasi-brittle properties of wood, but may still be improved. Indeed, the  
 291 rejected rate of 15% in mode I and 30% in mode II may be reduced by increasing the ligament length and by eliminating  
 292 every knot on the crack path. But this second point would drastically increase the needs in raw materials in order to  
 293 obtain specimens of clear wood long enough for the chosen geometry. And, in order to be in accordance with the on site  
 294 construction challenges, may be the knots should be taken into account into the statistic studies. Nevertheless, by using  
 295 this methodology, the R-curves parameters of two wood species (Maritime Pine and Spruce) have been determined  
 296 for two crack propagation mode (mode I and II). And, the differences of behaviour between those two species were  
 297 highlighted, with a more brittle behaviour for Spruce than for Maritime Pine. Moreover, contrary to the Spruce, the  
 298 Maritime Pine crack propagation in mode I showed a dependency to the crack orientation plane. The differences  
 299 between the mode I and the mode II crack propagations were also highlighted by this work, with a  $G_{Rc}$  2 to 4 times  
 300 higher in mode II than in mode I according to the wood species. And, the mode II of propagation appears more stable  
 301 than the mode I and less influenced by the other properties of the wood (density and crack plane orientation).

302 This study does not show a clear correlation between the wood density and the R-curves parameters. But, in the  
 303 case of the Maritime Pine, the dependency of the R-curve parameters to the crack plane orientation may create an  
 304 artificial variability which could hide a possible correlation. In order to eliminate any possible correlation between  
 305 the wood density and the R-curve parameters in mode I, an experimental campaign which investigates the influence

### Mode I and II R-curves characterization of the Maritime Pine and Spruce

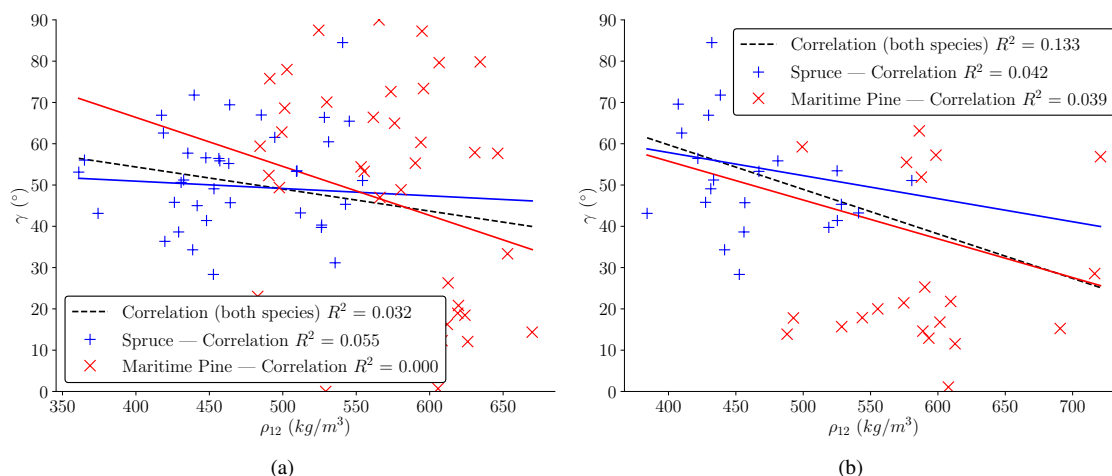


**Figure 13:** Correlations between the wood density and the crack orientation plane for both species for the mode I (a) and the mode II (b)

306 of the wood density for specific crack plane orientations should be carried out. Such experimental campaign should  
 307 also be carried out on other wood species in order to increase the density range investigated. Moreover, the differences  
 308 observed between only two wood species, which are both softwood, show the necessity to establish a data base of the  
 309 R-curves parameters for many wood species and more particularly for hardwood, by using a rigorous and systematic  
 310 methodology. To conclude, this study is another step to improve the methodology to characterize the quasi-brittle  
 311 behaviour of wood. In the future, in order to improve the characterization of the R-curve parameters, the focus should  
 312 be given to the determination of the plateau value  $G_{Rc}$ .

## References

- [1] Aicher, S., Böstrom, L., Girel, M., Kretschmann, D., Valentin, G., 1997. Determination of fracture energy of wood in Mode II: RILEM TC 133 report. Number 1997,13 in SP report / Swedish National Testing and Research Institute, Borås. OCLC: 246644740.
- [2] Bažant, Z.P., 2002. Concrete fracture models: testing and practice. *Engineering fracture mechanics* 69, 165–205.
- [3] Bažant, Z.P., Kazemi, M.T., 1990. Size effect in fracture of ceramics and its use to determine fracture energy and effective process zone length. *Journal of the American Ceramic Society* 73, 1841–1853.
- [4] Bazant, Z.P., Planas, J., 1997. *Fracture and size effect in concrete and other quasibrittle materials*. volume 16. CRC press.
- [5] Blank, L., Fink, G., Jockwer, R., Frangi, A., 2017. Quasi-brittle fracture and size effect of glued laminated timber beams. *European Journal of Wood and Wood Products* 75, 667–681.
- [6] Coureau, J.L., Morel, S., Dourado, N., 2013. Cohesive zone model and quasibrittle failure of wood: a new light on the adapted specimen geometries for fracture tests. *Engineering Fracture Mechanics* 109, 328–340.
- [7] Coureau, J.L., Morel, S., Gustafsson, P.J., Lespine, C., 2007. Influence of the fracture softening behaviour of wood on load-COD curve and R-curve. *Materials and Structures* 40, 97–106. URL: <http://www.springerlink.com/index/10.1617/s11527-006-9122-z>, doi:10.1617/s11527-006-9122-z.
- [8] Danielsson, H., Gustafsson, P.J., 2013. A three dimensional plasticity model for perpendicular to grain cohesive fracture in wood. *Engineering Fracture Mechanics* 98, 137–152.
- [9] Danielsson, H., Gustafsson, P.J., 2014. Fracture analysis of glued laminated timber beams with a hole using a 3d cohesive zone model. *Engineering Fracture Mechanics* 124, 182–195.
- [10] Daudeville, L., 1999. Fracture in spruce: experiment and numerical analysis by linear and non linear fracture mechanics. *Holz als Roh- und Werkstoff* 57, 425–432.
- [11] De Moura, M., Morais, J., Dourado, N., 2008. A new data reduction scheme for mode I wood fracture characterization using the double cantilever beam test. *Engineering Fracture Mechanics* 75, 3852–3865. URL: <http://linkinghub.elsevier.com/retrieve/pii/S0013794408000556>, doi:10.1016/j.engfracmech.2008.02.006.
- [12] De Moura, M., Oliveira, J., Morais, J., Xavier, J., 2010. Mixed-mode i/ii wood fracture characterization using the mixed-mode bending test. *Engineering Fracture Mechanics* 77, 144–152.
- [13] De Moura, M., Silva, M., De Morais, A., Morais, J., 2006. Equivalent crack based mode ii fracture characterization of wood. *Engineering Fracture Mechanics* 73, 978–993.
- [14] Dietsch, P., Winter, S., 2012. Eurocode 5—future developments towards a more comprehensive code on timber structures. *Structural Engineering International* 22, 223–231.

- [15] Dourado, N., Morel, S., de Moura, M.F.S.F., Valentin, G., Morais, J., 2008. Comparison of fracture properties of two wood species through cohesive crack simulations. *Composites Part A: Applied Science and Manufacturing* 39, 415–427. URL: <http://www.sciencedirect.com/science/article/pii/S1359835X07001704>, doi:10.1016/j.compositesa.2007.08.025.
- [16] Eurocode 5, 2004. Eurocode 5 : Design of timber structures - Part 1-1: General - Common rules and rules for buildings .
- [17] Guan, Z., Zhu, E., 2009. Finite element modelling of anisotropic elasto-plastic timber composite beams with openings. *Engineering Structures* 31, 394–403.
- [18] Gustafsson, P.J., 1988. A study of strength of notched beams, Parksville, Canada.
- [19] Jernkvist, L.O., 2001. Fracture of wood under mixed mode loading: I. derivation of fracture criteria. *Engineering Fracture Mechanics* 68, 549–563.
- [20] Jockwer, R., 2014. Structural behaviour of glued laminated timber beams with unreinforced and reinforced notches. Ph.D. thesis. ETH ZURICH. Zurich.
- [21] Jockwer, R., Steiger, R., Frangi, A., Jochen, K., 2011. Impact of material properties on the fracture mechanics design approach for notched beams in Eurocode 5. URL: [https://www.researchgate.net/profile/Rene\\_Steiger/publication/278672372\\_Impact\\_of\\_material\\_properties\\_on\\_the\\_fracture\\_mechanics\\_design\\_approach\\_for\\_notched\\_beams\\_in\\_Eurocode\\_5/links/5582b68c08aeab1e4667766e.pdf](https://www.researchgate.net/profile/Rene_Steiger/publication/278672372_Impact_of_material_properties_on_the_fracture_mechanics_design_approach_for_notched_beams_in_Eurocode_5/links/5582b68c08aeab1e4667766e.pdf).
- [22] Larsen, H., Gustafsson, P., 1991. The fracture energy of wood in tension perpendicular to the grain. errata, and annex a12 and a13 to cib paper w18a/23-19-2. results from a joint testing project, in: CIB W18 meeting 24, pp. 1–6.
- [23] Lartigau, J., 2013. Caractérisation du comportement des assemblages par goujons collés dans les structures bois. phdthesis. Université Sciences et Technologies - Bordeaux I. URL: <https://tel.archives-ouvertes.fr/tel-00922998/document>.
- [24] Lartigau, J., Coureau, J.L., Morel, S., Galimard, P., Maurin, E., 2015. Mixed mode fracture of glued-in rods in timber structures. *International Journal of Fracture* 192, 71–86.
- [25] Lespine, I., 2007. Influence de la géométrie des structures sur les propriétés de rupture dans les matériaux quasi-fragiles. Ph.D. thesis. Bordeaux I. URL: <http://www.theses.fr/2007BOR13533>.
- [26] Méité, M., Dubois, F., Pop, O., Absi, J., 2013. Mixed mode fracture properties characterization for wood by Digital Images Correlation and Finite Element Method coupling. *Engineering Fracture Mechanics* 105, 86–100. URL: <http://www.sciencedirect.com/science/article/pii/S0013794413000131>, doi:10.1016/j.engfracmech.2013.01.008.
- [27] Morel, S., 2007. R-curve and size effect in quasibrittle fractures: Case of notched structures. *International journal of solids and structures* 44, 4272–4290.
- [28] Morel, S., Dourado, N., Valentin, G., 2005. Wood: a quasibrittle material R-curve behavior and peak load evaluation. *International Journal of Fracture* 131, 385–400. URL: <http://link.springer.com/10.1007/s10704-004-7513-0>, doi:10.1007/s10704-004-7513-0.
- [29] Morel, S., Lespine, C., Coureau, J.L., Planas, J., Dourado, N., 2010. Bilinear softening parameters and equivalent lefm r-curve in quasibrittle failure. *International Journal of Solids and Structures* 47, 837–850.
- [30] Morel, S., Mourot, G., Schmittbuhl, J., 2003. Influence of the specimen geometry on r-curve behavior and roughening of fracture surfaces. *International Journal of Fracture* 121, 23–42.
- [31] Phan, N.A., 2016. Simulation of time-dependent crack propagation in a quasi-brittle material under relative humidity variations based on cohesive zone approach: application to wood. Ph.D. thesis. Bordeaux. URL: <http://www.theses.fr/2016BORD0008>.
- [32] Phan, N.A., Morel, S., Chaplain, M., 2016. Mixed-mode fracture in a quasi-brittle material: R-curve and fracture criterion – Application to wood. *Engineering Fracture Mechanics* 156, 96–113. URL: <http://www.sciencedirect.com/science/article/pii/S001379441630008X>, doi:10.1016/j.engfracmech.2016.02.006.
- [33] Sorin, E., 2018. Fissuration en modes mixtes dans le bois: diagnostic et évaluation des méthodes de renforcement local. Ph.D. thesis. Bordeaux.
- [34] Toussaint, E., Fournely, E., Moutou Pitti, R., Grédiac, M., 2016. Studying the mechanical behavior of notched wood beams using full-field measurements. *Engineering Structures* 113, 277–286. URL: <http://linkinghub.elsevier.com/retrieve/pii/S0141029616000766>, doi:10.1016/j.engstruct.2016.01.052.
- [35] Yoshihara, H., 2004. Mode II r-curve of wood measured by 4-enf test. *Engineering Fracture Mechanics* 71, 2065–2077.
- [36] Yoshihara, H., 2013. Initiation and propagation fracture toughness of solid wood under the mixed Mode I/II condition examined by mixed-mode bending test. *Engineering Fracture Mechanics* 104, 1–15. URL: <http://www.sciencedirect.com/science/article/pii/S0013794413001306>, doi:10.1016/j.engfracmech.2013.03.023.
- [37] Yoshihara, H., 2015. Mode II fracture mechanics properties of solid wood measured by the three-point eccentric end-notched flexure test. *Engineering Fracture Mechanics* 141, 140–151. URL: <http://www.sciencedirect.com/science/article/pii/S0013794415002258>, doi:10.1016/j.engfracmech.2015.05.028.